Cellular/Molecular

Decreased Temporal Precision of Auditory Signaling in *Kcna1*-Null Mice: An Electrophysiological Study *In Vivo*

Cornelia Kopp-Scheinpflug,[1,2] Katja Fuchs,[2] William R. Lippe,[1] Bruce L. Tempel,[1] and Rudolf Rübsamen[2]

[1]University of Washington, V. M. Bloedel Hearing Research Center and Department of Otolaryngology, Seattle, Washington 98195, and [2]Universtity of Leipzig, Institute of Zoology, 04103 Leipzig, Germany

The voltage-gated potassium (Kv) channel subunit Kv1.1, encoded by the *Kcna1* gene, is expressed strongly in the ventral cochlear nucleus (VCN) and the medial nucleus of the trapezoid body (MNTB) of the auditory pathway. To examine the contribution of the Kv1.1 subunit to the processing of auditory information, *in vivo* single-unit recordings were made from VCN neurons (bushy cells), axonal endings of bushy cells at MNTB cells (calyces of Held), and MNTB neurons of *Kcna1*-null (−/−) mice and littermate control (+/+) mice. Thresholds and spontaneous firing rates of VCN and MNTB neurons were not different between genotypes. At higher sound intensities, however, evoked firing rates of VCN and MNTB neurons were significantly lower in −/− mice than +/+ mice. The SD of the first-spike latency (jitter) was increased in VCN neurons, calyces, and MNTB neurons of −/− mice compared with +/+ controls. Comparison along the ascending pathway suggests that the increased jitter found in −/− MNTB responses arises mostly in the axons of VCN bushy cells and/or their calyceal terminals rather than in the MNTB neurons themselves. At high rates of sinusoidal amplitude modulations, −/− MNTB neurons maintained high vector strength values but discharged on significantly fewer cycles of the amplitude-modulated stimulus than +/+ MNTB neurons. These results indicate that in *Kcna1*-null mice the absence of the Kv1.1 subunit results in a loss of temporal fidelity (increased jitter) and the failure to follow high-frequency amplitude-modulated sound stimulation *in vivo*.

Key words: **voltage-gated potassium channel; Kv1.1; spike timing; cochlear nucleus; calyx of Held; MNTB; *in vivo* physiology**

Introduction

Voltage-gated potassium (Kv) channels play an important role in regulating the level of neuronal excitability, e.g., they shorten the duration of action potentials (APs) and help determine the frequency of repetitive firing and the timing of interspike intervals (Hille, 1992). *In vitro* studies in hippocampus (Smart et al., 1998), motor cortex (van Brederode et al., 2001), cerebellum (Zhang et al., 1999), and sciatic nerve (Zhou et al., 1998) suggest that removal of the Kv channel subunit Kv1.1 (encoded by the *Kcna1*gene) can cause subtle increases in neuronal excitability at many different sites in the nervous system. Mutation of *KCNA1* in humans is linked to episodic ataxia type 1, a disorder characterized by stress-induced ataxia and chronic muscle twitching (Browne et al., 1994). Affected persons also have a 10-fold higher likelihood of having epilepsy than does the general public (Zuberi et al., 1999).

The Kv1.1 subunit is strongly expressed in auditory nuclei, including the ventral cochlear nucleus (VCN) and the medial nucleus of the trapezoid body (MNTB) (Wang et al., 1994; Grigg et al., 2000). MNTB neurons receive excitatory input from bushy cells located in the contralateral VCN through large presynaptic terminals, the calyces of Held (Smith et al., 1991). MNTB neurons, in turn, form inhibitory synapses onto neurons of the medial and the lateral superior olive. AP timing in both of these nuclei is crucial for the encoding of interaural timing and level differences, related to the roles of the nuclei in sound localization. In the MNTB, specializations including low-threshold potassium currents and the specialized presynaptic calyces are thought to ensure minimal latency fluctuations and the preservation of timing (Trussell, 1999). *In vitro* studies of the VCN and the MNTB have suggested that the Kv1.1 subunit contributes to a low-threshold Kv current that leads to strong accommodation (firing of a single, short latency AP in response to prolonged depolarizing current steps) and to a limitation of temporal summation of synaptic inputs (Oertel, 1983; Manis and Marx, 1991; Brew and Forsythe, 1995; Trussell, 1999).

Recordings in brain slices from mice lacking the *Kcna1*gene (−/−) show that in absence of the Kv1.1 subunit, MNTB neurons change their firing pattern from a single AP in control (+/+) mice to a train of APs in −/− littermates (Brew et al., 2003). Furthermore, Gittelman et al. (2001) found that the time between a depolarizing current injection and the occurrence of the first spike was more variable in −/− than +/+ MNTB neurons. Although these studies suggest a role for Kv1.1 subunits in the regulation of excitability and AP timing in MNTB neurons *in vitro*, almost nothing is known about the role of the subunit in auditory information processing *in vivo*. Here we present our study of auditory processing in the brainstem based on single-

Received July 2, 2003; revised Aug. 15, 2003; accepted Aug. 15, 2003.

This work was supported by the Deutsche Forschungsgemeinschaft (KO 2207/1–1 and Ru 390–15/2) and the National Institutes of Health (DC 03805 and DC 04661). We thank Helen Brew and Josh Gittelman for helpful comments on a previous version of this manuscript. We are especially thankful to Linda Robinson for mouse care, breeding, and genotyping and to Tina Schwabe for technical assistance in some of the experiments.

Correspondence should be addressed to Cornelia Kopp-Scheinpflug, V. M. Bloedel Hearing Research Center and Department of Otolaryngology, University of Washington, Box 357923, Seattle, WA 98195. E-mail: connyks@u.washington.edu.

 0270-6474/03/239199-09$15.00/0

unit recordings in −/− mice and their +/+ controls *in vivo*. We used pure-tone sinusoids and sinusoidally amplitude-modulated signals to investigate the auditory processing of temporal information.

Portions of these results were presented in abstract form (Kopp-Scheinpflug et al., 2001, 2003b).

Materials and Methods

Mouse strains and genotyping

The experiments were performed at the Neurobiology Laboratories of the Zoological Department of the University of Leipzig (Germany) and at the V. M. Bloedel Hearing Research Center of the University of Washington (Seattle, WA). All experimental procedures were approved by the Saxonian District Government (Leipzig) as well as the University of Washington Institutional Animal Care and Use Committee and were performed in accordance with the National Institutes of Health Guide for the Care and Use of Laboratory Animals. The *Kcna1*^{tm1Tem} strain was generated as described in Smart et al. (1998). Chimerical founders were crossed and maintained in serial backcrosses to C3HeB/FeJ females freshly obtained from The Jackson Laboratory (Bar Harbor, ME). Mice used in this study were generated by intercrossing heterozygote from the C3HeB/FeJ-*Kcna1*^{tm1Tem} line at N7–N12 backcross generations maintained at the University of Washington and the University of Leipzig. Mice were maintained on a 12 hr light/dark cycle with food and water available *ad libitum*. Male and female mice aged 3–4 weeks and weighing 12–25 gm were used in the experiments.

Genotyping was performed on DNA isolated from tail clips of each mouse in a litter aged 7–10 d as described by Brew et al. (2003). Detailed protocols are available online (http://depts.washington.edu/tempelab/).

In vivo *electrophysiology*

Surgical preparation. During the experiments and the surgical preparation, the animals were anesthetized with an initial dose of 0.5 ml/100 gm body weight of a mixture of ketamine hydrochloride (41.7 mg/kg body weight; Parke-Davis, Courbevoie, France) and xylazine hydrochloride (2.3 mg/kg body weight; Bayer, Wuppertal, Germany). A constant level of anesthesia was maintained throughout the recording experiments by hourly injections of one-third of the initial dose. The skull of an experimental animal was exposed along the dorsal midsagittal line, and a small metal bolt for supporting the animal in the stereotaxic recording device was glued to the bone overlaying the forebrain. Two holes were drilled in the skull 2000–2300 μm caudal to the lambda suture, which correspond to positions above the rostral third of the cerebellum. The first drill hole, located 1500 μm lateral to the midline, was used to position the reference electrode in the superficial cerebellum. For the insertion of recording electrodes the second drill hole (500 μm diameter) was located over the midline, and the electrodes were angled at 28–30° to the midsagittal plane for the VCN and 5–8° for the MNTB.

Acoustic stimulation. The auditory stimuli presented included pure tones and sinusoidally amplitude-modulated (SAM) signals. Stimuli were digitally generated with 16 bit accuracy by a 486/33 computer. The stimuli were delivered at 250 kilosamples/sec per channel through a two-channel, 14 bit digital-to-analog converter including a custom-made low-pass resynthesis filter (50 kHz cutoff) and a software-controlled attenuator (0–120 dB in 1 dB steps). Sounds were delivered through EC1 electrostatic speakers (Tucker-Davis Technologies), which have small pipes onto which acoustic tubing was attached to deliver stimuli to the outer ear ~5 mm from the animal's eardrum. The frequency characteristic of the transducer was measured with a quarter inch condenser microphone (Bruel & Kjaer type 2619) coupled to a short plastic tube mimicking the conditions in the ear canal. A computer-controlled procedure determined for 50 frequencies per decade the sound pressure levels at a defined input voltage. The data were stored in a computer file that was used during experiments for online correction of stimulus intensities.

Data collection and analysis

All recording experiments were performed in a sound-attenuated chamber (type 400; Industrial Acoustics). Generally, each animal was used in two or three daily recording sessions, with each recording session lasting 5–6 hr. During the experiments the body temperature was kept between 36 and 37.5°C by positioning the animal on a temperature-controlled heating pad (Harvard Apparatus) and maintaining the temperature of the sound-attenuated chamber at 25–30°C. After daily recording sessions, the electrodes were removed, and the holes in the skull were reversibly closed with a clot of agarose.

Multiunit mapping. The procedures for mapping the borders of the nuclei were described in detail in a previous paper (Kopp-Scheinpflug et al., 2003a). In brief, at the beginning of the first recording session, stereotaxic coordinates of either the VCN or MNTB were determined by online analysis of acoustically evoked multiunit activity. Glass micropipettes (Clark Electromedical Instruments) filled with 3 M KCl and having impedances of 5–10 MΩ were used. Using monaural tone-burst stimulation, ipsilateral in VCN experiments and contralateral in MNTB experiments, the characteristic frequencies (CF) of multiunits were measured by a computer-automated procedure every 100 μm in several penetrations in the estimated position of the respective nuclei [test range 1.0–50 kHz and 0–90 dB sound pressure level (SPL)].

Single-unit recordings. After multiunit mapping, recordings from single units were made through higher impedance glass micropipettes (15–30 MΩ). The activity of isolated single units was bandpass filtered (0.3–10 kHz) and amplified to the voltage range of the spike discriminator and the analog-to-digital converter. Single units were identified by their relatively constant spike height and waveform and a large signal-to-noise ratio (>2). For acquisition of single-unit activity, the amplified recording signal was delivered to a custom-made window discriminator followed by an event-timer personal computer interface. The discriminated spike times were acquired with 100 μsec resolution using custom-written real-time computer programs (Dörrscheidt, 1981).

Analysis of spike recordings. The excitatory response map for each unit was measured by random presentation of pure-tone pulses (100 msec duration, 5 msec rise–fall time, 50 msec interstimulus interval) within a given matrix of 16 × 15 frequency–intensity pairs (240 combinations). Each frequency–intensity combination was presented five times in a predefined frequency–intensity array. The timing and the number of spikes were measured during the 100 msec period of stimulus presentation and in the absence of acoustic stimulation [spontaneous activity (SR)]. From these data the frequency–threshold curve, the CF, and the threshold at CF were calculated. Threshold was defined as the sound intensity at CF that, on a 10% significance level, caused an increase of firing rate above the spontaneous rate (Dörrscheidt, 1981; Kopp-Scheinpflug et al., 2003a). The first-spike latency of each unit was determined by presenting 50 repetitive CF tone bursts at 80 dB SPL. The latency analysis was done as suggested by Young et al. (1988) and was based on the first spike that occurred in response to each tone burst. The measures we used were the mean first-spike latency and the SD (jitter) of the first spike latencies. In units without spontaneous activity, the first spike in the response was taken to be the first spike occurring after the stimulus onset. In spontaneously active neurons, however, a spontaneous spike may occur after stimulus onset but before the first sound-evoked spike. To eliminate these spikes from the latency analysis, a cursor was aligned by eye on the beginning of the rise of the onset peak in the poststimulus time histogram (PSTH). Mean latency and jitter were computed from the first spike after the time marked by this cursor. A potential problem with this method is that the latency may be prolonged by refractoriness in cases in which a spontaneous spike occurs immediately before the cursor. To check the refractory effect, latency and jitter calculations were done in two ways: using the first spike after the cursor and using the first spike that followed the stimulus onset, including spontaneous spikes. These two measures differed by <4%.

The carrier frequency of the SAM signals was set at the CF of the unit and 80 dB SPL. All SAM signals were 100% modulated and had modulation rates that ranged between 20 and 1000 Hz. For analysis of the neuronal responses to SAM signals, the vector strength (VS) and entrainment were calculated. To exclude the contribution of the onset response to vector strength and entrainment, only the steady-state response (20–100 msec of the response) was included in the respective calculations. The vector strength, as originally introduced by Goldberg and Brown (1969), was used to quantify the degree of phase locking of the response

of a single unit to the phase of a pure tone sinusoidal stimulus. In the present study, VS was adopted to quantify the degree of phase locking to the envelope of a SAM signal. VS was calculated by the following equation:

$$VS = \sqrt{[\sum \sin(a)]^2 + [\sum \cos(a)]^2}/n,$$

in which a is the phase of an occurring spike, and n is the total number of spikes. A VS value of 1.0 indicates that all spikes occur at exactly the same phase of the stimulus envelope, whereas a VS value of 0.0 stands for spike firing that is independent of the signal waveform.

The entrainment (Phillips, 1989; Joris et al., 1994) describes the degree to which individual neurons entrain, i.e., fire at each cycle of a periodic acoustic stimulus. Entrainment is defined as percentage of stimulus cycles that evoke at least one spike. Perfect entrainment (100%) is achieved when a single spike occurs with each SAM stimulus cycle and the distribution of the interspike intervals (ISI) consists of a single peak at the period of the modulation frequency. Note that VS and entrainment refer to two different aspects of the timing of the response. Conceivably, a neuron can discharge perfectly in phase (VS = 1) but always skip one or more stimulus cycles, resulting in an entrainment of 0.

Statistical analyses of the data were performed with SigmaStat/SigmaPlot (SPSS Science, Chicago, IL). Unless indicated otherwise, results are expressed as mean ± SEM. For normally distributed data, statistical significance was assessed using the Student's t test or paired t test. For non-normal distributions, significance was assessed using the Wilcoxon Signed Rank Test or the Mann–Whitney Rank Sum Test.

Verification of recording sites. In each animal, all recording sites were verified histologically by marking with horseradish peroxidase (HRP). At the end of the recording session, the recording electrode was replaced with a glass micropipette filled with a solution of 9% HRP in 0.9% NaCl, which was injected iontophoretically (2 μA for 5 min) into the recording site. The position of the HRP electrode was confirmed by measuring the CF, threshold, and temporal response pattern of the neuronal activity at the injection site. The animal was allowed to survive for 24 hr. It was then deeply anesthetized with Na pentobarbital (1 gm/kg body weight, i.p.; Narcoren, Merieux, France) and perfused via the left ventricle of the heart with 0.9% NaCl solution followed by fixative (2.5% paraformaldehyde in 0.1 M phosphate buffer, pH 7.4) for 20–25 min. The brain was cut on a vibratome, and the 100 μm tissue sections were reacted using the 3, 3′-diaminobenzidine reaction to visualize the HRP mark (Adams, 1981). After staining with cresyl violet, the tissue sections were examined under the light microscope, and the electrode tracks and recording sites were reconstructed.

Results

Extracellular single-unit recordings were made from 93 units in the auditory brainstem of 24 mice: 10 *Kcna1*-nulls (−/−) and 14 littermate controls (+/+). Included are recordings from VCN neurons (+/+: $n = 12$; −/−: $n = 18$), from calyces of Held (+/+: $n = 7$; −/−: $n = 9$), and from MNTB neurons (+/+: $n = 25$; −/−: $n = 22$). For each unit the CF and the threshold were determined. In the VCN the CFs ranged between 1.6 and 39.8 kHz in +/+ mice and between 6.8 and 39.7 kHz in the −/− mice and were not significantly different between genotypes (Fig. 1*A*) ($p = 0.763$). The mean thresholds (± SEM) of VCN neurons (+/+: 30.0 ± 4 dB SPL; −/−: 31.9 ± 3 dB SPL) also did not differ significantly different between genotypes (Fig. 1*A*) ($p = 0.687$). The CFs of MNTB neurons ranged between 8.4 and 40.6 kHz in +/+ mice and between 12.5 and 26.5 kHz in the −/− mice and were also not significantly different between genotypes (Fig. 1*B*) ($p = 0.601$). The mean thresholds of MNTB neurons (+/+: 27.4 ± 3 dB SPL; −/−: 32.3 ± 2 dB SPL) did not differ significantly between genotypes (Fig. 1*B*) ($p = 0.144$).

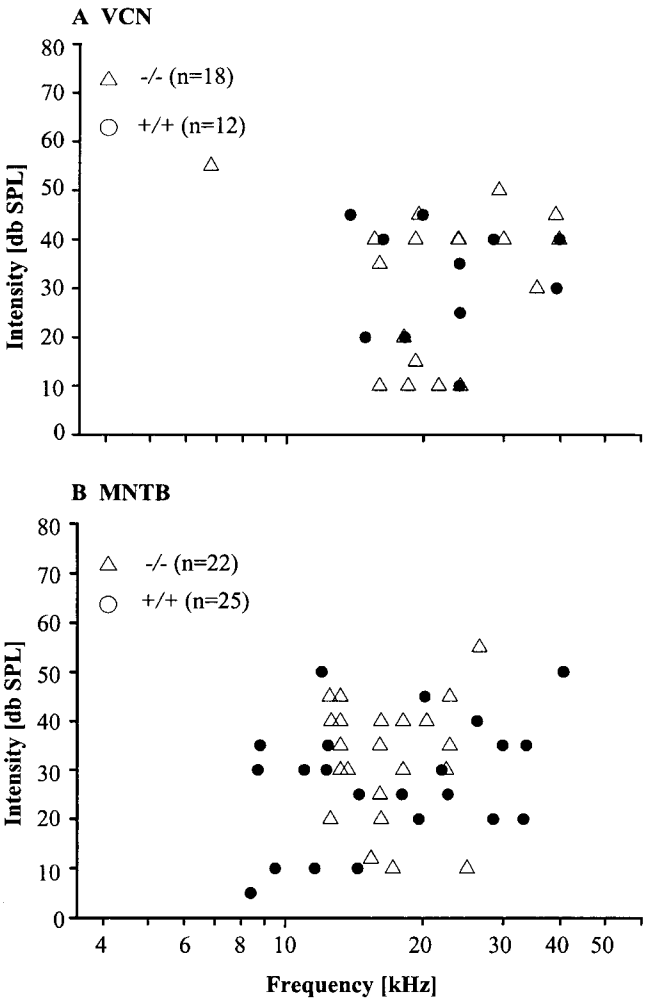

Figure 1. *A*, *B*, Distribution of CFs in the VCN (*A*) and in the MNTB (*B*). Note that units of both genotypes can have elevated thresholds. The lowest CF among the VCN units was 1.6 kHz. For a better visualization of the other CF values, this one outlier is not shown in the figure.

Firing rate

For each neuron the spontaneous rate and the sound-driven rate at CF were measured. Spontaneous rates were not significantly different between +/+ neurons and −/− neurons in both the VCN (+/+: 26.4 ± 11 spikes/sec; −/−: 19.6 ± 7 spikes/sec; $p = 0.597$) and MNTB (+/+: 35.9 ± 8 spikes/sec; −/−: 44.7 ± 9 spikes/sec; $p = 0.296$). However, a genotype-specific difference in firing rates at higher sound intensities can be clearly seen in the rate-level functions (RLFs) (Fig. 2). The RLFs of +/+ and −/− VCN neurons overlap over a wide intensity range (Fig. 2*A*) and become significantly different at levels ≥75 dB SPL (Fig. 2*B*). In the MNTB, the −/− RLFs are generally flatter than the +/+ RLFs (Fig. 2*C*). Whereas some +/+ and −/− RLFs have similar slopes and cover the same dynamic range, other +/+ RLFs reach higher firing rates over the entire range of intensities. The mean firing rate of +/+ MNTB neurons was significantly greater than −/− neurons at all intensities ≥45 dB SPL (Fig. 2*D*).

Comparison of Figure 2, *B* and *D*, shows that the reduction in discharge rates of −/− neurons compared with +/+ neurons began at lower sound intensities and was proportionally greater in the MNTB then in the VCN. This suggests that some factor in addition to the reduction in sound-evoked firing rate at the level

of the VCN contributed to the genotype-specific difference in firing rates of MNTB neurons. One possible source would be a higher rate of transmission failures at the calyx–MNTB synapse in −/− than in +/+ mice. To examine this, we simultaneously recorded the discharge activity of MNTB neurons and of their excitatory calyceal input (Kopp-Scheinpflug et al., 2003a). When measuring the firing rates of presynaptic calyces and postsynaptic MNTB neurons a failure rate, the percentage of calyceal discharges that fail to generate a postsynaptic spike (100% = presynaptic calyx discharges) can be calculated (Kopp-Scheinpflug et al., 2003a). The mean failure rates at the calyx–MNTB synapse at CF/80 dB SPL were 41% for +/+ mice ($n = 7$ neurons) and 37% for −/− mice ($n = 9$ neurons) and did not differ significantly between genotypes ($p = 0.569$). This suggests that the larger genotype-specific difference in firing rate that we found in MNTB did not primarily originate at the calyx–MNTB synapse.

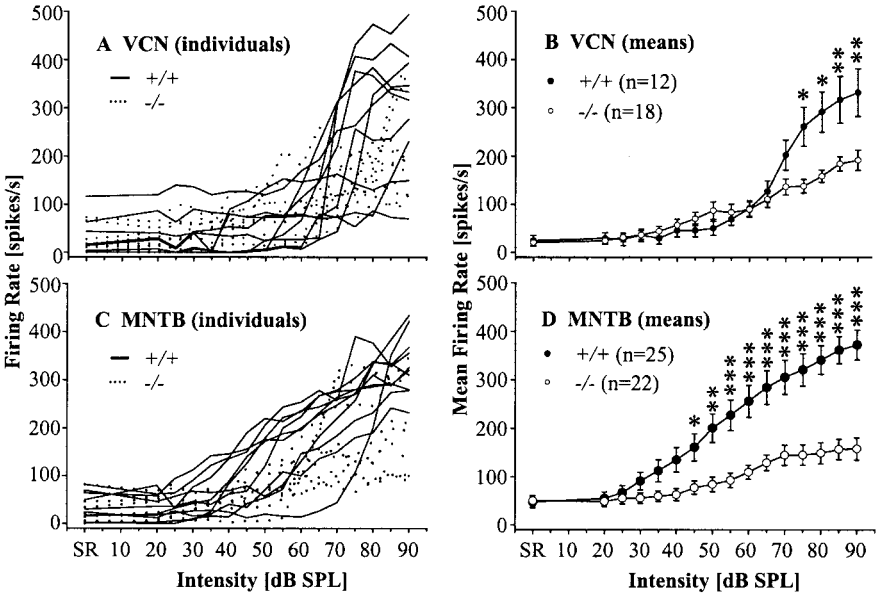

Figure 2. *A–D*, RLFs for representative (10 each) VCN (*A*) and MNTB (*C*) neurons in +/+ and −/− mice. The RLFs of −/− neurons (*A, C*, dotted lines) are flat compared with the RLFs of +/+ neurons (solid lines). Mean RLFs of all units in VCN (*B*) differ significantly only at SPLs ≥75 dB. Mean RLFs in MNTB (*D*) are significantly different at all intensities ≥45 dB SPL. Error bars indicate SEM. *$p \leq 0.05$; **$p \leq 0.005$.

Temporal response pattern

In response to tone bursts at CF/80 dB SPL, +/+ units in VCN and in MNTB had the typical primary-like or primary-like notch PSTHs described previously for the principal cells of these nuclei in many species (Fig. 3*A,C*) (cat: Pfeiffer, 1966; Guinan et al., 1972a,b; Smith et al., 1991; guinea pig: Winter and Palmer, 1990; chinchilla: Caspary and Finlayson, 1991; Caspary et al., 1993; Feng et al., 1994; gerbil: Feng et al., 1994; Tsuchitani, 1997; Kopp-Scheinpflug et al., 2002, 2003a). The PSTHs of the −/− units also consisted of a phasic onset component followed by a tonic response for the remainder of the stimulus (Fig. 3*B,D*). However, examination of the raster plots in the right columns and insets of Figure 3*A–D* shows that the first spikes in all 50 repetitions were much more aligned in the +/+ units than in the −/− units. This suggests that there was much more variation in the latency of the first spikes (Fig. 3*A–D*, insets) in the −/− units.

We examined the variation in latency for each unit by measuring their first-spike latency and the SD of the first-spike latency (jitter) to repetitive tone bursts at CF and sound intensities from the thresholds of the units up to 80 dB SPL. At 80 dB SPL the mean first-spike latencies of VCN neurons ranged from 2.5 to 4.8 msec in the +/+ mice and from 2.8 to 7.5 msec in the −/− mice (Fig. 4*A,B*). Although approximately one-third of the −/− VCN neurons had longer mean first-spike latencies (Fig. 4*C*) than the maximum latency of the +/+ neurons, on average latency did not differ significantly between genotypes (−/−: 4.6 ± 0.3 msec; $n = 18$ compared with +/+: 3.8 ± 0.2 msec; $n = 12$; $p = 0.169$) (Fig. 4*C*). In MNTB neurons, mean first-spike latency ranged from 2.7 to 7.1 msec (+/+) and from 4.7 to 11.9 msec (−/−) (Fig. 4*D–F*). Here, the first-spike latency was significantly shorter in +/+ mice (4.1 ± 0.3 msec; $n = 25$) compared with −/− mice (7.3 ± 0.4 msec; $n = 22$; $p \leq 0.001$) (Fig. 4*F*). Most notably, in both nuclei the jitter was greatly increased in −/− compared with +/+ neurons (VCN: 0.6 ± 0.1 vs 0.2 ± 0.02 msec; $p \leq 0.001$; MNTB: 4.2 ± 0.6 vs 0.9 ± 0.12 msec; $p \leq 0.001$) (Fig. 4*C,F*). In addition, the magnitude of increase was noticeably greater in the MNTB than in the VCN. The examination of first-spike latency and jitter at lower sound intensities led to exactly the same conclusions at all other intensities examined.

Because the difference in jitter between the +/+ genotype and the −/− genotype was much larger in the MNTB than in the VCN, we addressed the question of whether this difference originated during spike conductance along the VCN bushy cell axons or during synaptic transmission at the calyx–MNTB synapse or during the generation of APs in MNTB neurons. We examined this question by simultaneously recording the discharge activity of MNTB neurons and their excitatory calyceal input. In seven +/+ units and nine −/− units, the extracellular recordings yielded complex waveforms, in which a bipolar signal component indicated the postsynaptic action potential of an MNTB neuron and a preceding prepotential the discharge of its afferent calyceal input (Fig. 5*A*, inset). These recordings allowed direct comparisons between the response of a calyx and of the MNTB neuron that it contacted (Kopp-Scheinpflug et al., 2003a). The mean first-spike latencies measured at the calyces were significantly longer in −/− mice (6.4 ± 0.7 msec) than in +/+ mice (3.6 ± 0.3; $p = 0.001$) (Fig. 5*A,B*). Additionally, the jitter was significantly larger in the −/− calyces (3.7 ± 0.8 msec) than in +/+ calyces (0.8 ± 0.1 msec; $p = 0.008$) (Fig. 5*C*). The latency (+/+: 4.5 ± 0.5 msec; −/−: 7.8 ± 0.8 msec) and jitter (+/+: 0.9 ± 0.2 msec; −/−: 4.9 ± 1.1 msec) of the postsynaptic spikes in these simultaneous recordings (Fig. 5*D–F*) were comparable to the MNTB data reported above (Fig. 4*D–F*).

In all recording sites (VCN, calyces, and MNTB), the jitter was significantly larger in −/− mice than in +/+ controls. Although in both genotypes the major increase of the jitter occurred from the VCN to the calyces (Fig. 6), this increase was very small in the +/+ mice (0.5 ± 0.1 msec). In −/− mice, the mean increase in jitter from the VCN to the MNTB calyces was large (4.5 ± 1.2 msec; $p \leq 0.001$). Only a small additional increase was found postsynaptically in the MNTB neurons ($p = 0.667$).

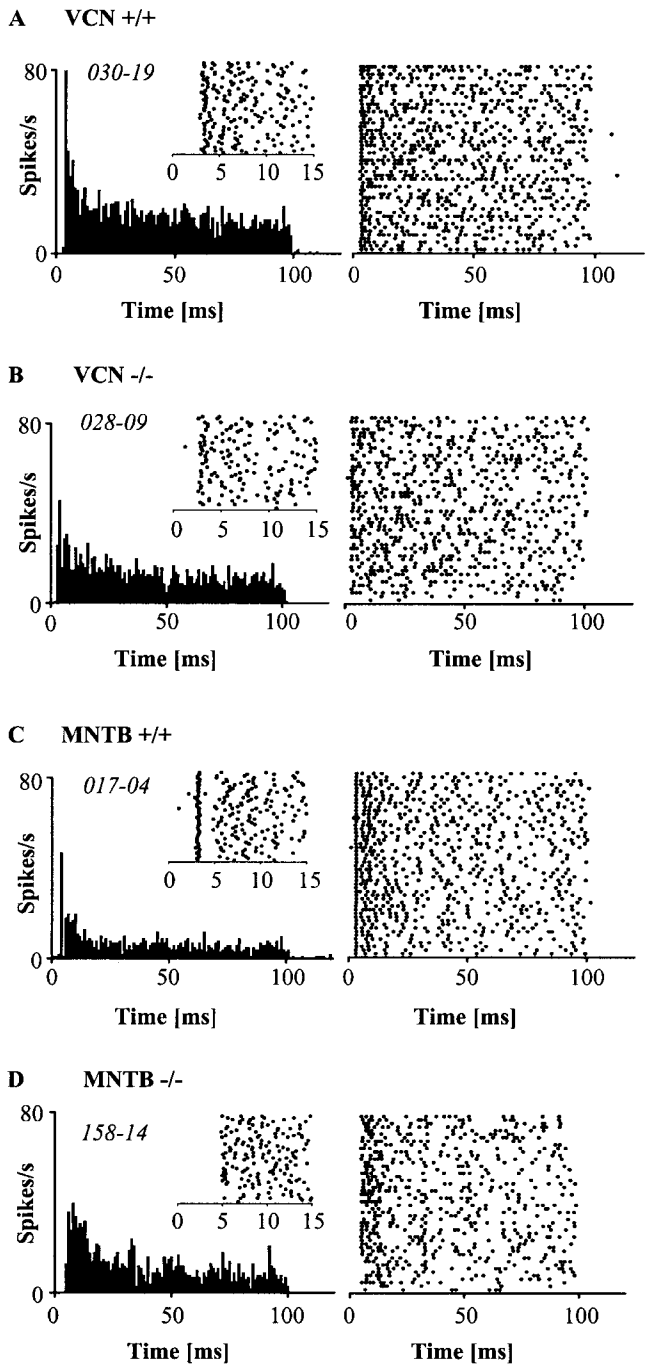

Figure 3. Dot raster displays and PSTHs of typical VCN and MNTB units of +/+ and −/− mice at CF/80 dB SPL, 100 msec tone burst, 50 stimulus repetitions. Left columns show PSTHs (bin width 1 msec). The right columns show dot raster displays of which the respective first 15 msec are given in the insets with an enlarged time scale. *A*, +/+ VCN neuron; *B*, +/+ MNTB neuron; *C*, −/− VCN neuron; *D*, −/− MNTB neuron. Note that the latency of the first spike in the onset response (inset) is more variable in the −/− neurons than in the +/+ neurons.

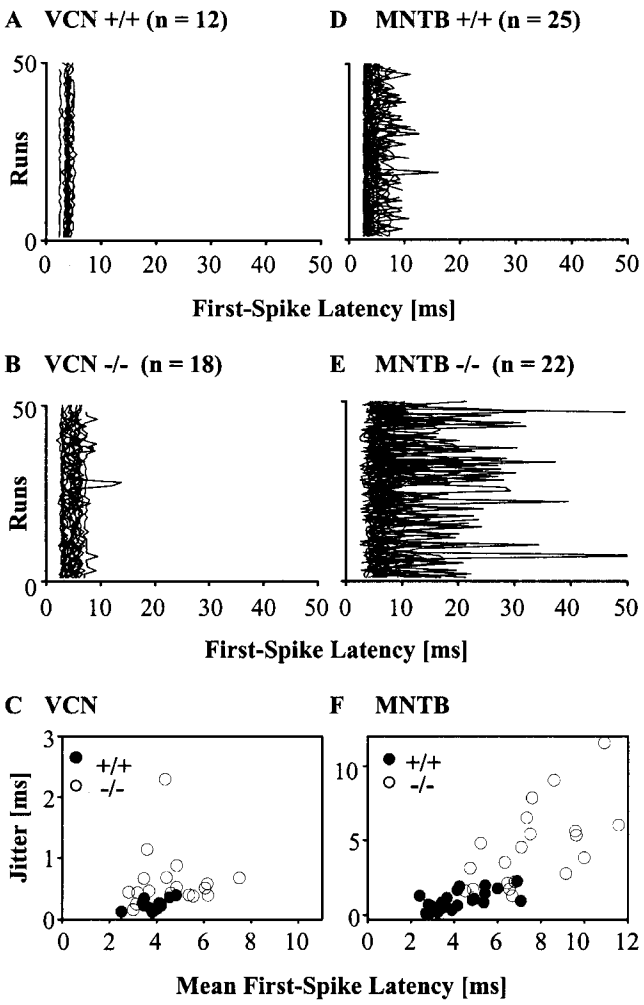

Figure 4. *A–F*, First-spike latencies (50 stimulus presentations) of single neurons in the VCN (*A*, *B*) and in the MNTB (*D*, *E*). Each unit is represented by a different line. A unit with no jitter at all would be represented by a straight vertical line. "Noisier" lines reflect more jitter. The jitter of each single neuron, quantified by the SD of the first-spike latency (see Materials and Methods), is plotted versus its absolute latency in *C* and *F*. Notice the prominent increase in the MNTB mean latency and jitter in the −/− mice. Spontaneous spikes were excluded from this analysis (see Materials and Methods for details).

Responses to acoustic transients

The results above demonstrate the influence of a lack of channels containing Kv1.1 subunits on the onset response of auditory brainstem neurons. How is the processing of temporal information during the sustained (steady-state) response of units affected by the lack of the Kv1.1 subunit? To answer this, the ability of VCN and MNTB neurons to phase-lock to the envelope of SAM signals was analyzed. A vector strength value of 0.3 was chosen as a cutoff criterion for classifying a response to SAM as being phase-locked. Of the 49 neurons in our sample that were tested for SAM responses, 80% [VCN: $n = 8/11$ (+/+) and $n = 12/13$ (−/−); MNTB: $n = 12/14$ (+/+) and $n = 7/11$ (−/−)] phase-locked to SAM rates as high as 800 Hz (VCN) and as high as 1000 Hz (MNTB). Representative examples of the phase-locked responses of +/+ MNTB neurons and −/− MNTB neurons are shown in Figure 7. The cyclic peaks in the PSTHs (Fig. 7*A*,*C*) show that both neurons strongly phase-locked at modulation frequencies at least up to 800 Hz. In the examples shown here, the +/+ unit has somewhat higher VS values at low modulation rates (100 and 200 Hz) than the −/− unit. But across the whole population of 12 +/+ units and 7 −/− units, the vector strength was not significantly different between MNTB units of both genotypes (Fig. 8*B*) ($p = 0.453$). VCN neurons also showed phase-locked responses to SAM stimuli, and their vector strength values also did not significantly differ between genotypes (Fig. 8*A*) ($p = 0.684$).

We also examined the degree to which VCN and MNTB neurons of both genotypes entrained, i.e., discharged at each cycle of

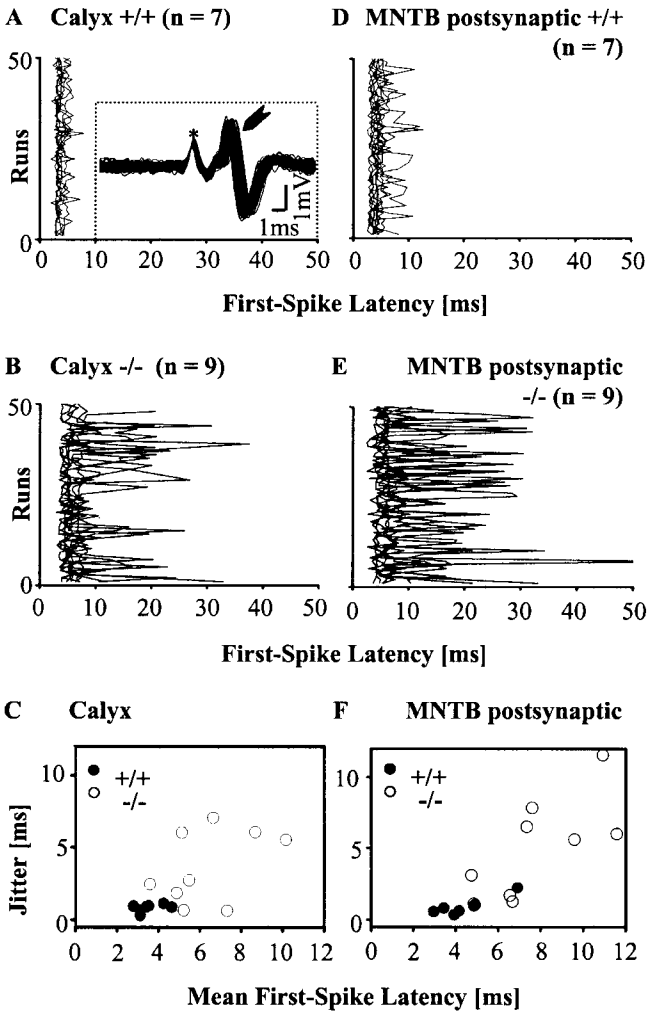

Figure 5. *A–F*, First-spike latencies of presynaptic responses (calyces) (*A, B*) and the corresponding postsynaptic responses of MNTB neurons acquired in simultaneous recordings (*D, E*). Each unit is represented by a different line. Mean first-spike latencies are 0.69 msec (+/+) and 1.17 msec (−/−) longer in the MNTB compared with the calyx. The inset in *A* shows an example of 77 superimposed waveforms of simultaneously recorded presynaptic (asterisk) and postsynaptic discharges (arrowhead) of an MNTB unit. *C, F*, The jitter of first-spike latencies in +/+ and −/− neurons is plotted versus their absolute latency.

an amplitude-modulated tone. The ISI histograms indicate the degree to which these MNTB neurons responded to every cycle of the SAM stimulus (Fig. 7*B,D*). If the cell responds to every cycle with exactly one spike, only one peak occurs in the ISI histogram at the period of the SAM stimulus. For example, the MNTB neuron in Figure 7*B* responded at almost every cycle to an SAM stimulation of 600 Hz. Multiple peaks in the ISI histogram indicate missing spikes in some cycles of the ongoing SAM stimulus and thus decreased entrainment. Although the two units shown in Figure 7 have comparable VS values at higher modulation rates, the entrainment was much better in the +/+ neurons, as indicated by the fewer number of peaks in the ISI histograms and the higher entrainment values. Compared across all MNTB neurons, the entrainment in −/− mice was significantly decreased compared with the wild types (Fig. 8*D*). In the +/+ MNTB, neurons showed ≥50% entrainment up to modulation rates of 800–1000 Hz, whereas in the −/− neurons the entrainment was already decreased to 50% at a modulation frequency of 200 Hz. In VCN neurons, entrainment did not differ significantly between +/+ and −/− mice (Fig. 8*C*) ($p = 0.840$).

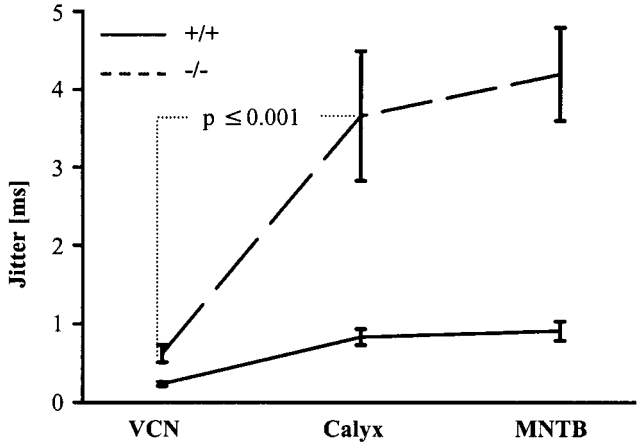

Figure 6. Distribution of jitter along the ascending auditory pathway (VCN, calyces, MNTB) in +/+ and −/− mice. In both genotypes the jitter increases from VCN to the calyces. This increase is much greater in −/− mice than in +/+ mice.

Discussion

The present study examined the contribution of the Kv1.1 potassium channel subunit to signal processing by auditory brainstem neurons *in vivo*. We found that thresholds and spontaneous firing rates of VCN and MNTB neurons were not different between genotypes. At middle-to-high-level sound intensities, however, the evoked firing rate was significantly decreased in VCN and MNTB neurons of −/− mice. In addition, jitter of the first-spike latencies in the −/− mice was larger than that in their +/+ littermates. MNTB neurons of −/− mice missed cycles at high SAM rates, while maintaining a high degree of phase-locking.

Firing rate

Our data show that the *in vivo* firing rate of VCN and MNTB neurons in *Kcna1*-null mice is maintained at spontaneous activity and decreased at higher intensities compared with +/+ controls. This contrasts with *in vitro* studies suggesting that removal of the *Kcna1* gene causes increased neuronal activity (Smart et al., 1998; Zhou et al., 1998; Zhang et al., 1999; Brew et al., 2003). However, the hyperexcitability reported in these studies was shown mostly at room temperature and was considerably increased when temperature was further reduced (Zhou et al., 1998). In our experiments, the body temperature of the mice was kept at 37.5–38°C, which might limit any cold-induced hyperexcitability.

Neurons of the VCN and MNTB are characterized by low-voltage activated potassium currents (Oertel, 1983; Manis and Marx, 1991; Brew and Forsythe, 1995; Trussell, 1999) and show very precise encoding of temporally structured acoustic signals. In slice preparations, the absence of the Kv1.1 subunit, which is normally strongly expressed in these neurons (Wang et al., 1994; Grigg et al., 2000), led to a 50% reduction in the low-voltage activated potassium current and to a doubling of the number of spikes in −/− MNTB neurons (Brew et al., 2003). Typically, both MNTB and VCN bushy cells fire only one or a few APs at the start of prolonged depolarizing current steps (Manis and Marx, 1991; Forsythe and Barnes-Davies, 1993; Brew and Forsythe, 1995) and are then silenced by the Kv1.1 containing channels (Dodson et al., 2002). The low firing incidence of these neurons may have made intrinsic hyperexcitability clearly detectable *in vitro*. *In vivo*, however, neuronal firing reflects both the intrinsic excitability of the neuron and the integration of its inhibitory and excitatory inputs.

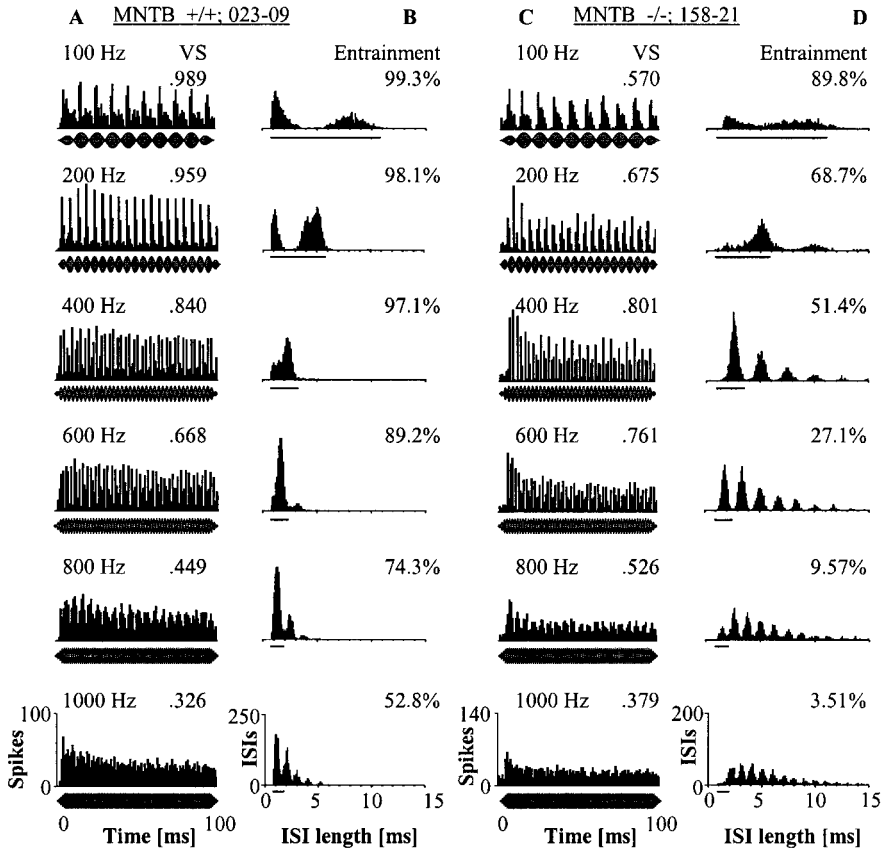

Figure 7. *A–D*, Response to SAM stimuli. Two representative examples of +/+ MNTB neurons (*A, B*) and −/− MNTB neurons (*C, D*). PSTHs (*A, C*) show the phase locking to the respective modulation frequencies. The envelope of the SAM stimulus is shown below each PSTH. Although the +/+ unit has somewhat higher VS values at low modulation rates (100 and 200 Hz) then the −/− unit, on average the VS is not significantly different between genotypes. ISI histograms (*B, D*) reflect the ability of the units to follow each cycle of the SAM sound. The length of each respective period is indicated by the bars below the histograms. The early peaks at 100 and 200 Hz in *B* represent ISIs shorter than the length of one period. This indicates that the neuron fires more than one spike per cycle. Entrainment is given in numbers (see Materials and Methods for further detail).

Thus, the +/+-like spontaneous rates and the decreased sound-evoked rates of −/− neurons at higher intensities could result from an adaptive upregulation of inhibitory transmitter systems. Indeed, cortical motor neurons from *Kcna1*−/− mice show an upregulation of GABAergic input from inhibitory interneurons (van Brederode et al., 2001). In addition to an upregulation of inhibition, it should also be considered that in +/+ VCN bushy cells and +/+ MNTB cells the Kv1.1 containing channels may underlie the current that limits the opportunity for the temporal summation of synaptic inputs (Oertel, 1983; Manis and Marx, 1991; Brew and Forsythe, 1995). The absence of this subunit in −/− neurons might lead to prolonged temporal summation of inhibitory inputs, particularly at higher intensities, in which inhibition is known to be more prominent both in VCN and in MNTB (Winter et al., 1990; Kopp-Scheinpflug et al., 2002, 2003a).

Temporal precision of spikes

The present data showed that the latency and the variability of the first spike were significantly increased in −/− VCN and MNTB neurons, both of which are thought to convey temporally precise afferent information in the +/+ controls. The results of the presynaptic calyceal recordings suggest that the increased jitter measured postsynaptically in −/− MNTB neurons arises not predominantly in MNTB neurons, but in the axons of VCN neurons or the calyces or both. The fact that Kv1.1 subunits have not been detected in the membrane of calyces of bushy cell axons in +/+ mice (Brew et al., 2003) suggests that the main source for the increase in jitter is the bushy cell axon. One potential source of jitter produced in axons, in particular in the nodal membrane, is the sodium channel fluctuation near or below spike threshold (Rubinstein, 1995). One way in which the Kv1.1 containing channels may reduce jitter in axonal conduction is by stabilizing the membrane potential (V_m) at rest. It is known that very slight changes (noise) in the axonal resting V_m reliably alter conduction velocity (for review, see Stys and Waxman, 1994). Because the internodal Kv1 channels are open at or near rest, they may function to limit V_m noise. Axons of the Kv1.1 −/− neurons may have less of this stabilizing current, and therefore experience more V_m noise, which would then result in more temporal jitter in the first spike.

The situation may be different for ongoing spike firing. During high-frequency firing, e.g., throughout SAM stimulation, the membrane may never be at rest, or Kv-channels not containing the Kv1.1 subunit may provide this stabilizing function. Certainly, the precision of spike timing, as measured by the vector strength, was not different between genotypes in VCN bushy cells and in MNTB cells. Using the entrainment as a measure, the −/− MNTB neurons but not the −/− VCN neurons showed lower values than the respective +/+ controls. One reason for the preserved entrainment of spikes in −/− VCN units could be the high degree of afferent summation. Globular bushy cells in the murine VCN receive input from up to four auditory nerve fibers (Oertel, 1985) and therefore have a higher safety factor. In contrast, MNTB neurons depend primarily on a single excitatory calyceal input. The reduction in entrainment of −/− MNTB neurons might be caused by alterations in signal transmission along the bushy cell axon and/or signal transduction at the calyx. Chiu et al. (1999) suggested that at axonal transition zones, e.g., at branch points or toward the axon terminal, an impedance match is achieved by increasing the sodium current per unit length. As a result, the excitability of the myelinated nerve segment should increase just ahead of the transition zones, a process that in +/+ fibers might be damped by Kv1.1 containing channels. In −/− mice, transition zones were markedly destabilized, which caused nerve back firing (for review, see Chiu et al., 1999). In the bushy cell axon there are two branch points that have to be regarded in the present context. Before the fiber forms the calyx, it sends off (1) collateral projections to the VNTB and (2) precalyceal collaterals heading for neighboring MNTB cells. Cases of calyceal collaterals have also been described (Kuwabara et al., 1991). Thus, including the calyx itself, there are three to four transition zones along the bushy cell axon, which in −/− mice all might destabilize the axonal membrane. At high firing rates, e.g., during our SAM stimulation experiments, the destabilization of the membrane potential might lead to failures in spike propagation.

Functions of Kv1.1 in mouse auditory brainstem neurons

Our data show that the Kv1.1-containing channels are especially important to maintain short latency and low variability in the first-spike response. The latency of the first spike in response to a relevant stimulus and the jitter of first-spike latency (in this respect a measure of "noise in the latency code") have been suggested to jointly provide a neuronal code in the auditory system (Phillips and Hall, 1990; Brugge et al., 1996; Heil and Irvine, 1997; Eggermont, 1998; Furukawa et al., 2000).

Why is the first spike so important? We know that transient, rapidly transmitted, and precisely timed spike activity in the auditory brainstem is essential for detection of acoustic signals and localization of the sources (Batra et al., 1993; Grothe, 1994; Joris and Yin, 1998). This should become particularly difficult when the relevant neuronal information occurs intermingled with activity that can be characterized as stochastic (irrelevant) noise. Precisely timed, across-frequency processing might be one mechanism by which coherent activity is isolated from stochastic noise.

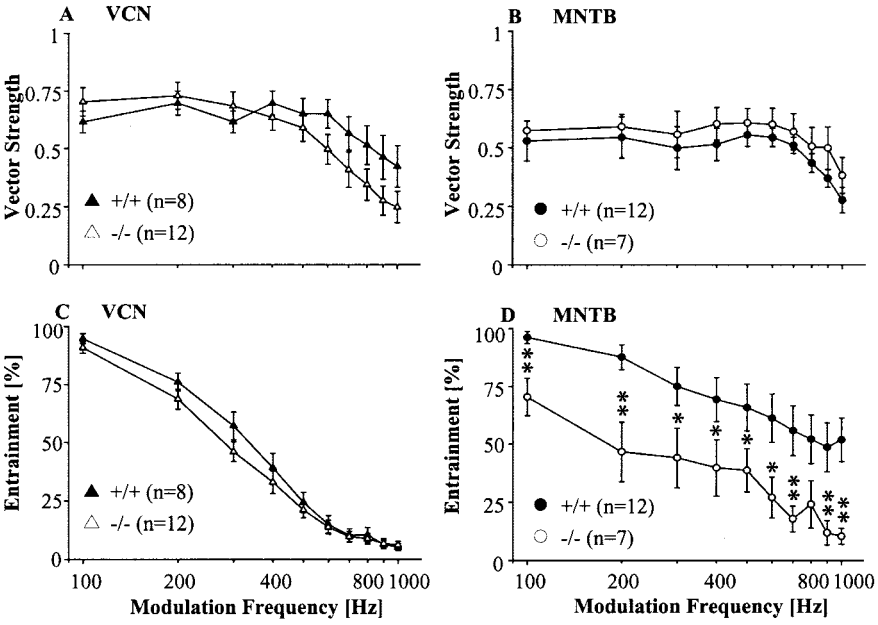

Figure 8. Vector strength and entrainment as a function of modulation frequency for VCN (*A, C*) and MNTB (*B, D*) neurons of +/+ and −/− mice. In both nuclei, vector strengths (*A, B*) typically decreased with increasing modulation frequency, but there was no significant difference between genotypes. In the VCN (C) the entrainment also decreased with increasing modulation frequency but did not differ between genotypes. *D*, +/+ MNTB neurons (closed circles) show significantly higher entrainment than −/− MNTB neurons (open circles) up to 1000 Hz modulation frequency. Error bars indicate SEM. $*p \leq 0.05$; $**p \leq 0.005$.

In addition to limiting spike jitter, Kv1.1-containing channels support the reliable encoding of fast repetitive transients. Given their role in the temporal precision of AP firing, it seems likely that Kv1.1-containing channels contribute to the refinement of many different types of auditory discrimination tasks. Behavioral tests on Kcna1-null mice, such as those of Allen et al. (2003) showing deficits in sound localization, should provide further understanding of the role of Kv1.1-containing channels.

References

Adams JC (1981) Heavy metal intensification of DAB-based HRP reaction product [letter]. J Histochem Cytochem 29:775.

Allen PD, Bell J, Dargani N, Moore CA, Tyler CM, Ison JR (2003) Kcna1 knockout mice have a profound deficit in discriminating sound source location, Neuroscience Meeting, New Orleans, LA, November.

Batra R, Kuwada S, Stanford TR (1993) High-frequency neurons in the inferior colliculus that are sensitive to interaural delays of amplitude-modulated tones: evidence for dual binaural influences. J Neurophysiol 70:64–80.

Brew HM, Forsythe ID (1995) Two voltage-dependent K+ conductances with complementary functions in postsynaptic integration at a central auditory synapse. J Neurosci 15:8011–8022.

Brew HM, Hallows JL, Tempel BL (2003) Hyperexcitability and reduced low threshold potassium currents in auditory neurons of mice lacking the channel subunit Kv1.1. J Physiol (Lond) 548:1–20.

Browne DL, Gancher ST, Nutt JG, Brunt ER, Smith EA, Kramer P, Litt M (1994) Episodic ataxia/myokymia syndrome is associated with point mutations in the human potassium channel gene, KCNA1. Nat Genet 8:136–140.

Brugge JF, Reale RA, Hind JE (1996) The structure of spatial receptive fields of neurons in primary auditory cortex of the cat. J Neurosci 16:4420–4437.

Caspary DM, Finlayson PG (1991) Superior olivary complex: functional neuropharmacology of the principal cell types. In: Neurobiology of hearing: the central auditory system (Altschuler BM, Clopton BM, Bobbin RP, and Hoffman DW, eds), pp 141–193. New York: Raven.

Caspary DM, Palombi SP, Backoff PM, Helfert RH, Finlayson PG (1993) GABA and Glycine inputs control discharge rate within the excitatory response area of primarylike and phaselocked AVCN neurons. In: The mammalian cochlear nuclei: organization and function (Merchan MA, ed). New York: Plenum.

Chiu SY, Zhou L, Zhang CL, Messing A (1999) Analysis of potassium channel functions in mammalian axons by gene knockouts. J Neurocytol 28:349–364.

Dodson PD, Barker MC, Forsythe ID (2002) Two heteromeric Kv1 potassium channels differentially regulate action potential firing. J Neurosci 22:6953–6961.

Dörrscheidt GH (1981) The statistical significance of the peristimulus time histogram (PSTH). Brain Res 220:397–401.

Eggermont JJ (1998) Azimuth coding in primary auditory cortex of the cat. II. Relative latency and interspike interval representation. J Neurophysiol 80:2151–2161.

Feng JJ, Kuwada S, Ostapoff EM, Batra R, Morest DK (1994) A physiological and structural study of neuron types in the cochlear nucleus. I. Intracellular responses to acoustic stimulation and current injection. J Comp Neurol 346:1–18.

Forsythe ID, Barnes-Davies M (1993) The binaural auditory pathway: membrane currents limiting multiple action potential generation in the rat medial nucleus of the trapezoid body. Proc R Soc Lond B Biol Sci 251:143–150.

Furukawa S, Xu L, Middlebrooks JC (2000) Coding of sound-source location by ensembles of cortical neurons. J Neurosci 20:1216–1228.

Gittelman J, Brew HM, Tempel BL (2001) KCNA channels help regulate the timing of action potentials in MNTB neurons, Abstract 693, Midwinter Meeting of the Association for Research in Otolaryngology, St. Petersburg Beach, FL, February.

Goldberg JM, Brown PB (1969) Response of binaural neurons of dog superior olivary complex to dichotic tonal stimuli: some physiological mechanisms of sound localization. J Neurophysiol 32:613–636.

Grigg JJ, Brew HM, Tempel BL (2000) Differential expression of voltage-gated potassium channel genes in auditory nuclei of the mouse brainstem. Hear Res 140:77–90.

Grothe B (1994) Interaction of excitation and inhibition in processing of pure tone and amplitude-modulated stimuli in the medial superior olive of the mustached bat. J Neurophysiol 71:706–721.

Guinan Jr JJ, Guinan SS, Norris BE (1972a) Single auditory units in the superior olivary complex I: responses to sounds and classification based on physiological properties. Int J Neurosci 4:101–120.

Guinan Jr JJ, Norris BE, Guinan SS (1972b) Single auditory units in the superior olivary complex II: locations of unit categories and tonotopic organization. Int J Neurosci 4:147–166.

Heil P, Irvine DR (1997) First-spike timing of auditory-nerve fibers and comparison with auditory cortex. J Neurophysiol 78:2438–2454.

Hille B (1992) Ionic channels of excitable membranes. Sunderland, MA: Sinauer.

Joris PX, Yin TCT (1998) Envelope coding in the lateral superior olive. III. Comparison with afferent pathways. J Neurophysiol 79:253–269.

Joris PX, Smith PH, Yin TC (1994) Enhancement of neural synchronization in the anteroventral cochlear nucleus. II. Responses in the tuning curve tail. J Neurophysiol 71:1037–1051.

Kopp-Scheinpflug C, Lippe WR, Rubsamen R, Tempel BL (2001) Decreased temporal precision of auditory signaling in Kcna1-null mice: an electrophysiological study in vivo, Abstract 694, Midwinter Meeting of the Association for Research in Otolaryngology, St. Petersburg Beach, FL, February.

Kopp-Scheinpflug C, Dehmel S, Dorrscheidt GJ, Rubsamen R (2002) Interaction of excitation and inhibition in anteroventral cochlear nucleus neurons that receive large endbulb synaptic endings. J Neurosci 22:11004–11018.

Kopp-Scheinpflug C, Lippe WR, Dorrscheidt GJ, Rubsamen R (2003a) The medial nucleus of the trapezoid body in the gerbil is more than a relay: comparison of pre- and postsynaptic activity. J Assoc Res Otolaryngol 4:1–23.

Kopp-Scheinpflug C, Fuchs K, Lippe WR, Tempel BL, Rubsamen R (2003b) Increased jitter in first-spike latency in MNTB neurons of mice lacking the Kcna1 gene is probably caused by increased variability in axonal and/or calyceal conduction, Abstract 373, Midwinter Meeting of the Association for Research in Otolaryngology, Daytona Beach, FL, February.

Kuwabara N, DiCaprio RA, Zook JM (1991) Afferents to the medial nucleus of the trapezoid body and their collateral projections. J Comp Neurol 314:684–706.

Manis PB, Marx SO (1991) Outward currents in isolated ventral cochlear nucleus neurons. J Neurosci 11:2865–2880.

Oertel D (1983) Synaptic responses and electrical properties of cells in brain slices of the mouse anteroventral cochlear nucleus. J Neurosci 3:2043–2053.

Oertel D (1985) Use of brain slices in the study of the auditory system: spatial and temporal summation of synaptic inputs in cells in the anteroventral cochlear nucleus of the mouse. J Acoust Soc Am 78:328–333.

Pfeiffer RR (1966) Classification of response patterns of spike discharges for units in the cochlear nucleus: tone-burst stimulation. Exp Brain Res 1:220–235.

Phillips DP (1989) Timing of spike discharges in cat auditory cortex neurons: implications for encoding of stimulus periodicity. Hear Res 40:137–146.

Phillips DP, Hall SE (1990) Response timing constraints on the cortical representation of sound time structure. J Acoust Soc Am 88:1403–1411.

Rubinstein JT (1995) Threshold fluctuations in an N sodium channel model of the node of Ranvier. Biophys J 68:779–785.

Smart SL, Lopantsev V, Zhang CL, Robbins CA, Wang H, Chiu SY, Schwartzkroin PA, Messing A, Tempel BL (1998) Deletion of the K(V)1.1 potassium channel causes epilepsy in mice. Neuron 20:809–819.

Smith PH, Joris PX, Carney LH, Yin TC (1991) Projections of physiologically characterized globular bushy cell axons from the cochlear nucleus of the cat. J Comp Neurol 304:387–407.

Stys PK, Waxman SG (1994) Activity-dependent modulation of excitability: implications for axonal physiology and pathophysiology. Muscle Nerve 17:969–974.

Trussell LO (1999) Synaptic mechanisms for coding timing in auditory neurons. Annu Rev Physiol 61:477–496.

Tsuchitani C (1997) Input from the medial nucleus of trapezoid body to an interaural level detector. Hear Res 105:211–224.

van Brederode JF, Rho JM, Cerne R, Tempel BL, Spain WJ (2001) Evidence of altered inhibition in layer V pyramidal neurons from neocortex of Kcna1-null mice. Neuroscience 103:921–929.

Wang H, Kunkel DD, Schwartzkroin PA, Tempel BL (1994) Localization of Kv1.1 and Kv1.2, two K channel proteins, to synaptic terminals, somata, and dendrites in the mouse brain. J Neurosci 14:4588–4599.

Winter IM, Palmer AR (1990) Temporal responses of primarylike anteroventral cochlear nucleus units to the steady-state vowel /i. J Acoust Soc Am 88:1437–1441.

Winter IM, Robertson D, Yates GK (1990) Diversity of characteristic frequency rate-intensity functions in guinea pig auditory nerve fibres. Hear Res 45:191–202.

Young ED, Robert JM, Shotner WP (1988) Regularity and latency of units in the ventral cochlear nucleus: implications for unit classification and generation of response properties. J Neurophysiol 60:1–29.

Zhang CL, Messing A, Chiu SY (1999) Specific alteration of spontaneous GABAergic inhibition in cerebellar Purkinje cells in mice lacking the potassium channel Kv1. 1. J Neurosci 19:2852–2864.

Zhou L, Zhang CL, Messing A, Chiu SY (1998) Temperature-sensitive neuromuscular transmission in Kv1.1 null mice: role of potassium channels under the myelin sheath in young nerves. J Neurosci 18:7200–7215.

Zuberi SM, Eunson LH, Spauschus A, De Silva R, Tolmie J, Wood NW, McWilliam RC, Stephenson JP, Kullmann DM, Hanna MG (1999) A novel mutation in the human voltage-gated potassium channel gene (Kv1.1) associates with episodic ataxia type 1 and sometimes with partial epilepsy. Brain 122:817–825.